

# NONLINEAR DYNAMICS ISSUES FOR QUASI-ISOCHRONOUS STORAGE RINGS \*

D. Jeon, M. Bai, C. M. Chu, X. Kang, S. Y. Lee, A. Riabko, X. Zhao  
Indiana University Cyclotron Facility  
2401 Milo B. Sampson Lane, Bloomington, IN 47405

*Abstract*

The synchrotron equation of motion in quasi-isochronous (QI) storage rings was transformed to a universal Weierstrass equation, where solution is given by Jacobian elliptic functions. Scaling properties of QI Hamiltonian were derived. The effects of phase space damping and the sensitivity of particle motion to external harmonic modulation were studied. We found that rf phase modulation is particularly enhanced in QI storage rings. This means that the operators of QI storage rings should pay special attention to rf phase modulation. Exact formula and sum rules for resonance strength coefficients were derived. In the presence of radiation damping and rf phase modulation, QI system exhibits a sequence of period-two bifurcation enroute towards global chaos (instability) in a region of modulation tune. The critical modulation amplitude for the onset of global chaos shows a cusp as a function of modulation tune. This cusp was shown to arise from the transition from the 2:1 to the 1:1 parametric resonances. We also studied the effect of rf voltage modulation and found that the tolerance of rf voltage modulation is much larger than that of rf phase modulation.

## 1 INTRODUCTION

Very short electron bunches, e.g. sub-millimeter in bunch length, can be important for such applications as time resolved experiments, next generation light sources, coherent synchrotron radiation, and damping rings for the next linear colliders. A possible method for producing short bunches is to reduce the phase slip factor  $\eta$  or the momentum compaction factor  $\alpha_c$  for electron storage rings because beam bunch width is proportional to  $\sqrt{|\eta_0|}$  for small bunches inside the bucket. Thus a short bunch regime is equivalent to the condition of a small  $|\eta_0|$ . Since  $\eta$  is related to the the revolution frequency deviation (see Eq. (1)), the condition of small  $|\eta|$  is also called the quasi-isochronous (QI) condition. Because of its potential benefit, interest in the physics of low  $\alpha_c$  lattice have recently grown [1-7]. This paper is a review of [8, 9]. The aspects of stochastic dynamics of QI system was also studied [10].

Including the velocity difference between the off momentum particle and the synchronous particle, the fraction deviation of the revolution frequency is given by

$$\frac{\Delta\omega}{\omega_0} = -\eta\delta = -(\eta_0 + \eta_1\delta + \dots)\delta, \quad (1)$$

\* Work supported by DOE, Grant No. DOE-DE-FG02-93ER40801, and the NSF, Grant No. PHY-9512832.

where  $\eta_0$  and  $\eta_1$  are the first order and the second order phase slip factors and where  $\delta = \Delta p/p_0$ . For most of storage rings, the truncation of the phase slip factor at the  $\eta_1$  term is a good approximation.

Using  $(\phi, \delta)$  as conjugate phase space coordinates, where  $\phi$  is the rf phase angle, synchrotron mapping equations are given by

$$\delta_{n+1} = \delta_n + \frac{eV}{\beta^2 E} [\sin(\phi_{n+1} + \phi_s) - \sin \phi_s] - 2\pi\lambda\delta_n, \quad (2)$$

$$\phi_{n+1} = \phi_n + 2\pi h(\eta_0\delta_{n+1} + \eta_1\delta_{n+1}^2), \quad (3)$$

where the subscript stands for the revolution number,  $V$  is the rf voltage,  $h$  is the harmonic number,  $\phi_s$  is the synchronous phase, and  $\lambda$  is the damping decrement. Under QI condition,  $\eta_1\delta^3$  term is not negligible and should be included. Neglecting the friction term, the difference equation can be cast into the Hamiltonian given by

$$H = \frac{1}{2}h\eta_0\delta^2 + \frac{1}{3}h\eta_1\delta^3 + \frac{eV}{2\pi\beta^2 E} [\cos(\phi + \phi_s) + \phi \sin \phi_s], \quad (4)$$

$$\approx \frac{1}{2}h\eta_0\delta^2 + \frac{1}{3}h\eta_1\delta^3 - \frac{eV \cos \phi_s}{4\pi\beta^2 E} \phi^2, \quad (5)$$

where  $\theta = s/R$  serves as the time coordinate, and  $R$  is the mean radius of the storage ring.

## 2 PARTICLE HAMILTONIAN IN QI STORAGE RINGS

For synchrotron storage rings operating near the isochronous condition, the small amplitude synchrotron tune is given by

$$\nu_s = \sqrt{\frac{heV|\eta_0 \cos \phi_s|}{2\pi\beta^2 E_0}}, \quad (6)$$

where  $\beta c$  and  $E_0$  are the velocity and the energy of the beam. Using  $t = \nu_s\theta$  as the time variable and using  $(x, p)$  as the conjugate phase space coordinates, where

$$x = -\frac{\eta_1}{\eta_0} \frac{\Delta p}{p_0}, \quad p = \frac{dx}{dt}, \quad (7)$$

the synchrotron Hamiltonian for particle motion in QI storage rings is given by

$$H = \frac{1}{2}p^2 + \frac{1}{2}x^2 - \frac{1}{3}x^3. \quad (8)$$

The “energy”  $E$  of the autonomous Hamiltonian is a constant of motion with  $E \in [0, \frac{1}{6}]$  for particles inside the bucket. Figure 1 shows the potential energy and the stable bucket area for the Hamiltonian.

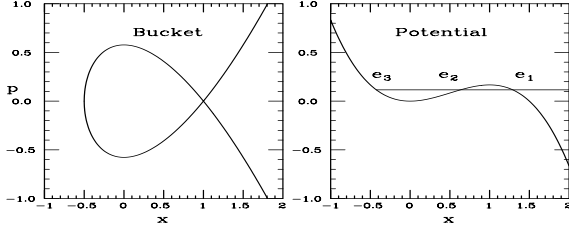


Figure 1: Stable bucket on the left and the potential energy.

The equation of motion for a particle with energy  $E$  is given by

$$\left(\frac{dx}{dt}\right)^2 = \frac{2}{3}x^3 - x^2 + 2E. \quad (9)$$

Letting  $u = \frac{1}{\sqrt{6}}t$  and  $\wp = x$ , the equation of motion is transformed to the standard Weierstrass equation:

$$\left(\frac{d\wp(u)}{du}\right)^2 = 4(\wp - e_1)(\wp - e_2)(\wp - e_3), \quad (10)$$

where the turning points,  $e_1 \geq e_2 \geq e_3$ , are given by

$$\begin{aligned} e_1 &= \frac{1}{2} + \cos(\xi), \quad e_2 = \frac{1}{2} + \cos(\xi - 120^\circ), \\ e_3 &= \frac{1}{2} + \cos(\xi + 120^\circ), \quad \xi = \frac{1}{3} \arccos(1 - 12E). \end{aligned}$$

For particles inside the separatrix, the discriminant is positive, i.e.  $\Delta = 648E(1 - 6E) > 0$ , and the Weierstrass  $\wp$  function can be expressed in terms of the Jacobian elliptic function:

$$x(t) = e_3 + (e_2 - e_3) \operatorname{sn}^2\left(\sqrt{\frac{e_1 - e_3}{6}} t | m\right), \quad (11)$$

$$m = \frac{e_2 - e_3}{e_1 - e_3} = \frac{\sin \xi}{\sin(\xi + 60^\circ)} \leq 1. \quad (12)$$

The period and the tune of the elliptic function are given by

$$T = 2\sqrt{6} \frac{K(m)}{\sqrt{e_1 - e_3}}, \quad Q = \frac{2\pi}{T} = \frac{\pi[\sqrt{3} \sin(\xi + 60^\circ)]^{1/2}}{\sqrt{6}K(m)}. \quad (13)$$

In the original accelerator coordinate system, the synchrotron tune becomes

$$Q_s = \nu_s Q = \nu_s \frac{\pi[\sqrt{3} \sin(\xi + 60^\circ)]^{1/2}}{\sqrt{6}K(m)}. \quad (14)$$

Figure 2 shows  $Q(E)$  as a function of energy. In particular, we note that the synchrotron tune decreases to zero very sharply near the separatrix, which causes parametric resonances induced by the time dependent perturbation to overlap one another and gives rise to chaos.

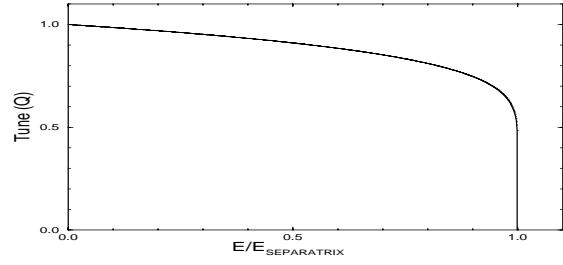


Figure 2: Tune  $Q$  as a function of  $E$ .

## 2.1 Action-angle variables

The action of a Hamiltonian torus is:

$$J = \frac{1}{8} \sqrt{\frac{2}{3}} (e_2 - e_3)^2 (e_1 - e_3)^{1/2} F\left(\frac{2}{3}, -\frac{1}{2}; 3; m\right), \quad (15)$$

where  $F\left(\frac{2}{3}, -\frac{1}{2}; 3; m\right)$  is a hypergeometric function given by

$$F\left(\frac{2}{3}, -\frac{1}{2}; 3; m\right) = 1 - \frac{1}{4}m - \frac{5}{128}m^2 - \frac{7}{512}m^3 - \dots$$

Using the generating function

$$F_2 \equiv \int_{e_3}^x p dx, \quad (16)$$

the angle variable is given by:

$$\psi = \frac{\partial F_2}{\partial J} = \sqrt{\frac{6}{e_1 - e_3}} Q F(w|m) = Qt, \quad (17)$$

where  $Q$  is the synchrotron tune given by Eq. (13) and  $F(w|m)$  is the incomplete elliptic integral of the first kind given by:

$$F(w|m) = \int_0^w \frac{dz}{\sqrt{1 - m \sin^2 z}}, \quad w = \arcsin \sqrt{\frac{x - e_3}{e_2 - e_3}}. \quad (18)$$

## 2.2 The bucket area

The bucket area is the area in phase space in which charged particles can be accelerated without loss. So the bigger the bucket area is, the more charged particles can be accelerated. The bucket area  $A$  in  $(x, p)$  is

$$A = 2\pi J_{sep} = \oint_{sep} p dx = \frac{6}{5}. \quad (19)$$

Thus the bucket area  $A_B$  in  $(\phi, \delta)$  is given by

$$A_B = \frac{6}{5} \left(\frac{|\eta_0|^{5/2}}{|\eta_1|^2}\right) \left(\frac{2\pi h \beta^2 E}{eV |\cos \phi_s|}\right)^{1/2}. \quad (20)$$

In contrast to the nominal synchrotron Hamiltonian, the bucket area of the QI Hamiltonian increases with *decreasing* rf voltage  $V$  and  $|\cos \phi_s|$ . Note also that the bucket area is proportional to  $|\eta_0|^{5/2}/|\eta_1|^2$ . For a lattice with a small  $\eta_0$ , a proper correction for  $\eta_1$  becomes necessary in order to provide a stable phase space for the beam bunch.

### 3 DYNAMICS WITH RF PHASE MODULATION

#### 3.1 Without damping

In the presence of rf phase modulation and without damping, the Hamiltonian is given by

$$H = \frac{p^2}{2} + \frac{x^2}{2} - \frac{x^3}{3} + \omega_m B x \cos \omega_m t, \quad (21)$$

$$= H_0 + \omega_m B x \cos \omega_m t, \quad (22)$$

where the effective modulation amplitude is

$$B = \frac{\eta_1 a}{\eta_0 \nu_s} \sim \frac{|\eta_1|}{|\eta_0|^{3/2}}, \quad (23)$$

$\omega_m = \nu_m / \nu_s$  is the normalized modulation tune,  $a$  and  $\nu_m$  are the rf phase modulation amplitude and tune. Note that  $B$  is greatly enhanced for QI storage rings.

##### 3.1.1 Expansion of phase space coordinates

$x$  can be expressed as a function of  $(J, \psi)$  as follows:

$$x(t) = g_0(J) + \sum_{n=1}^{\infty} g_n(J) \cos(n\psi), \quad (24)$$

where

$$\begin{aligned} g_0 &= e_3 + (e_1 - e_3) \frac{K(m) - E(m)}{K(m)}, \\ g_n &= (e_1 - e_3) \frac{2\pi^2}{K^2(m)} \frac{(-1)^n n q^n}{1 - q^{2n}}, \\ q &= e^{-\pi K'/K} = \frac{m}{16} + 8 \left(\frac{m}{16}\right)^2 + 84 \left(\frac{m}{16}\right)^3 + \dots, \\ \psi &= \frac{\pi}{2K(m)} \sqrt{\frac{e_1 - e_3}{6}} \nu_s \theta = Q \nu_s \theta = Qt, \end{aligned} \quad (25)$$

where  $K(m)$  and  $E(m)$  are the complete elliptic integrals of the first and second kind and  $K'(m) = K(1-m)$ .

The expansion coefficients satisfy the sum rule:

$$\sum_{n=1}^{\infty} g_n^2(J) = 2g_0(1 - g_0). \quad (26)$$

Since  $g_0 = 1$  on the separatrix, the strength of all harmonics must vanish on the separatrix.

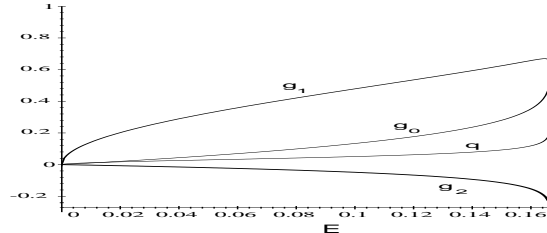


Figure 3: Plot of  $g_0, g_1, g_2$  and the parameter  $q$ .  $g_1$  is related with the 1:1 parametric resonance and  $g_2$  with the 2:1 resonance. As is predicted by sum rule, all the strength functions go to zero at the separatrix.

#### 3.1.2 Whisker map

Since  $Q(E)$  drops sharply near the separatrix, all the parametric resonances  $n : l$  satisfying  $\omega_m \approx \frac{n}{l} Q(E_{n:l})$  overlap near the separatrix, thus forming a stochastic layer. The width of stochastic layer can be estimated using the whisker map.

The energy change rate due to the time-dependent perturbation is given by

$$\frac{dH_0}{dt} = \frac{\partial H_0}{\partial t} + [H_0, H] = -\omega_m B p \cos \omega_m t. \quad (27)$$

Using the separatrix orbit:

$$x_{sx}(t) = 1 - \frac{3}{\cosh t + 1}, \quad p_{sx}(t) = \frac{3 \sinh t}{(\cosh t + 1)^2}, \quad (28)$$

the energy change in one complete revolution is given by

$$\begin{aligned} \Delta E &= -\omega_m B \int_{-\infty}^{\infty} p_{sx}(t - t_0) \cos \omega_m t dt \\ &= \frac{6\pi\omega_m^3 B}{\sinh \pi\omega_m} \sin \phi, \end{aligned} \quad (29)$$

where  $\phi = \omega_m t_0$ . The revolution period near the separatrix is given by

$$T(E) = 2\sqrt{\frac{6}{e_1 - e_3}} K(m) \approx \ln \left( \frac{144}{|\frac{1}{6} - E|} \right). \quad (30)$$

Thus the whisker map is given by

$$E_{n+1} = E_n + \frac{6\pi\omega_m^3 B}{\sinh \pi\omega_m} \sin \phi_n, \quad (31)$$

$$\phi_{n+1} = \phi_n + \omega_m \ln \left( \frac{144}{|\frac{1}{6} - E_{n+1}|} \right). \quad (32)$$

Related figure might be found (Fig. 3) in [9] which is omitted for limitation on space. The width of stochastic layer, estimated from the linearized whisker map, is

$$\left| E - \frac{1}{6} \right| \leq \frac{3\pi\omega_m^4 B}{2 \sinh \pi\omega_m}.$$

#### 3.2 With damping

Including damping force, the equation of motion becomes:

$$x'' + Ax' + x - x^2 = -\omega_m B \cos \omega_m t, \quad (33)$$

where

$$A = \frac{\lambda}{\nu_s} = \frac{U_0 J_E}{2\pi E_0 \nu_s} \sim \frac{1}{|\eta_0|^{1/2}}, \quad B = \frac{\eta_1 a}{\eta_0 \nu_s} \sim \frac{|\eta_1|}{|\eta_0|^{3/2}}. \quad (34)$$

It is worth pointing out that both the damping coefficient  $A$  and the phase modulation amplitude  $B$  are amplified as a result of scaling of the transformation into normalized phase space coordinates, because for QI storage rings, the value of  $|\eta_0|$  is orders of magnitude smaller than the usual storage rings.

### 3.2.1 Melnikov integral method

The Melnikov integral method has often been applied to study the chaotic transition of many dynamical systems. If the stable and unstable orbits from a hyperbolic fixed point cross each other, the dynamical system becomes homoclinic, which is an indicator of chaotic motion. Calculating the distance between the two orbits perturbatively, the Melnikov integral becomes

$$D = - \int_{-\infty}^{\infty} [\omega_m B p_{sx}(t - t_0) \cos \omega_m t - A p_{sx}^2(t - t_0)] dt, \quad (35)$$

where  $x_{sx}$  and  $p_{sx}$  are the separatrix orbit. After integration, it becomes:

$$D = - \frac{6\pi\omega_m^3 B \sin \omega_m t_0}{\sinh \pi\omega_m} - \frac{6A}{5}, \quad (36)$$

and the condition for global chaos is

$$B_{cr} = \frac{A \sinh \pi\omega_m}{5\pi \omega_m^3}. \quad (37)$$

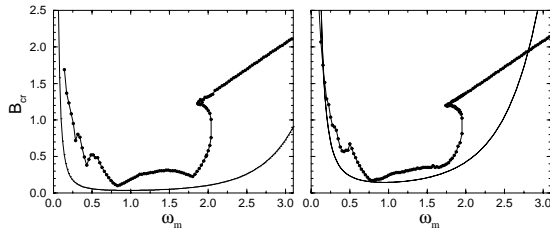


Figure 4:  $B_{cr}$  for  $A = 0.05$  (on the left) and for  $A = 0.2$ . Solid line is for Melnikov integral method and solid circle for numerical simulation.

The Melnikov integral method provides only a rough estimation for low modulation frequency  $\omega_m \leq 2$ . For high modulation frequency, it overestimates the stable region of parameter space. In short, the Melnikov integral method is a measure of rough estimation only for low modulation frequency.

### 3.2.2 Attractor solution for 1:1 parametric resonance

The attractor solution for the 1:1 parametric resonance can be obtained by harmonic linearization method. Let the ansatz be :

$$x = X_0 + X_1 \cos(\omega_m t + \xi_1), \quad (38)$$

then the following relations are obtained:

$$\omega_m^2 B^2 = A^2 \omega_m^2 X_1^2 + \left( \omega_m^2 - \sqrt{1 - 2X_1^2} \right)^2 X_1^2, \quad (39)$$

$$\tan \xi_1 = \frac{-A\omega_m}{\omega_m^2 - \sqrt{1 - 2X_1^2}}, \quad (40)$$

$$X_0 = \frac{1}{2} \left( 1 - \sqrt{1 - 2X_1^2} \right). \quad (41)$$

It should be noted that  $X_1 = \frac{1}{\sqrt{2}}$  represents the maximum oscillation amplitude for which this dynamical system is stable. Setting the maximum tolerable modulation amplitude for the 1:1 parametric resonance is given by

$$B_{cr,1:1} = \frac{1}{\sqrt{2}} \sqrt{A^2 + \omega_m^2}. \quad (42)$$

This is almost a linear function of  $\omega_m$  for large  $\omega_m$ .

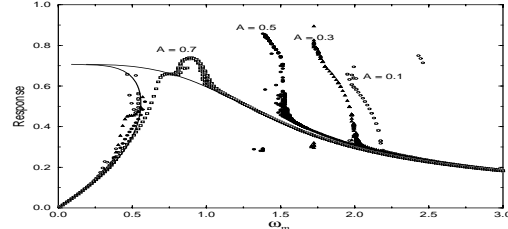


Figure 5:  $X_1$  obtained numerically for modulation amplitude  $B = 0.5$  with damping parameter  $A = 0.1, 0.3, 0.5$ , and  $0.7$  respectively. Solid lines correspond to the solution of Eq. (39) for  $A = 0.7$  and  $B = 0.5$ . Two characteristic features are (1) the threshold tune of the 2:1 parametric resonance decreases with increasing damping parameter  $A$ , and (2) the appearance of very strong stop band around  $\omega_m \approx 1$  for the 1:1 resonance.

### 3.2.3 Attractor solution for 2:1 parametric resonance

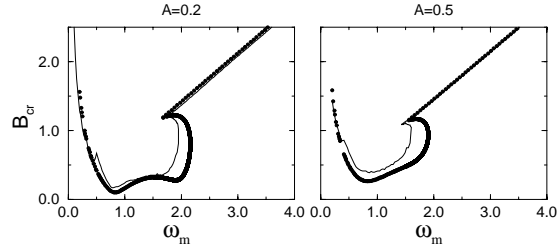


Figure 6: Plot of critical modulation amplitude  $B_{cr}$  for  $A = 0.2$  (left) and  $A = 0.5$  (right). Solid circles of boot-shape are obtained from 1:1 Eq. (39) and 2:1 Eq. (46) resonances and solid circles of straight line from Eq. (42). Thin solid line from numerical simulation.

The periodic attractor solution associated with the 2:1 parametric resonance can be obtained by using the ansatz:

$$x(t) = X_0 + X_1 \cos(\omega_m t + \xi_1) + y(t). \quad (43)$$

The equation of motion for  $y(t)$  is then given by

$$y'' + Ay' + [1 - 2X_0 - 2X_1 \cos(\omega_m t + \xi_1)] y \approx 0. \quad (44)$$

Let the solution of this damped Mathieu equation be

$$y(t) = X_{1/2}(s) \cos\left(\frac{\omega_m}{2} t + \xi_{1/2}\right). \quad (45)$$

The condition for Mathieu instability can also be obtained by assuming  $X_{1/2} \sim e^{st}$  with  $s \geq 0$ , i.e.

$$A^2 \frac{\omega_m^2}{4} + \left( \frac{\omega_m^2}{4} - \sqrt{1 - 2X_1^2} \right)^2 \leq X_1^2. \quad (46)$$

The boot-shaped curve (in solid circle) describes the onset of period-two bifurcation (Mathieu instability) obtained from Eq. (39) and setting equality to Eq. (46). The “straight line” defining the maximum tolerable modulation amplitude  $B_{cr}$  is in well agreement with the curve of Eq. (42). In conclusion, the stability of QI storage ring is determined mainly by the 1:1 and 2:1 parametric resonances. And it should be noted that the “cusp” structure is reproduced from the theory of these two resonances.

### 3.2.4 Chaos through period-two bifurcation

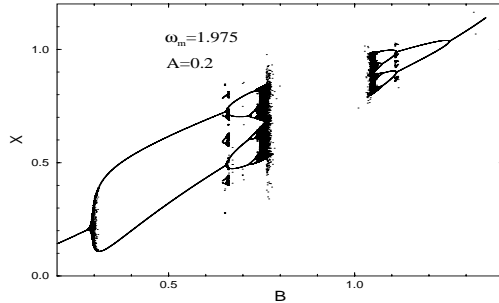


Figure 7: The attractors as a function of modulation amplitude  $B$  at the modulation frequency  $\omega_m = 1.975$  and the damping coefficient  $A = 0.2$ .

The upper “mirror” structure corresponds to the “cusp” structure in Fig. 4. This clearly shows chaos through a series of period-two bifurcation and this phenomenon occurs only for  $\omega_m \leq 2$  due to 2:1 parametric resonance. Systematic patterns of bifurcation are observed. Clearly period-two bifurcation can be attributed to 2:1 parametric resonance and occurs in the vicinity of this particular parametric resonance, i.e.,  $\omega_m \leq 2 + \epsilon$  where  $\epsilon$  is a small positive number.

## 4 DYNAMICS WITH RF VOLTAGE MODULATION

In the presence of rf voltage modulation and damping force, the equations of motion in normalized phase space are

$$p' = x - x^2, \quad x' = -p - bp \cos \omega_v t - Ax, \quad (47)$$

where

$$\frac{\Delta V}{V} = b \cos \omega_v t. \quad (48)$$

The Melnikov integral method was applied again to study the chaotic transition, which is given by

$$\begin{aligned} D &= \int_{-\infty}^{\infty} (x_{sx}(t) - x_{sx}^2(t)) [bp_{sx}(t) \cos \omega_v(t + t_0) \\ &+ Ap_{sx}(t)] dt, \quad (49) \\ &= \frac{3\pi \sin \omega_v t_0}{4 \sinh \pi \omega_v} b \omega_v^2 (\omega_v^2 + 1) (1 - \omega_v^2) + \frac{6A}{5}, \quad (50) \end{aligned}$$

where  $x_{sx}$  and  $p_{sx}$  are the separatrix orbit. The condition for a homoclinic structure near the separatrix is given by

$$b_{cr} = \frac{2A \sinh \pi \omega_v}{\pi \omega_v^2 (\omega_v^2 + 1) |\omega_v^2 - 1|}. \quad (51)$$

It should be pointed out that the dynamical system is infinitely stable for the modulation frequency of  $\omega_v \approx 1$ .

Numerical simulation revealed that QI system is very stable against voltage modulation. Due to limited space, interested readers are asked to refer to [9] for detailed discussion and figure (Fig. 12). Like the phase modulation, the Melnikov integral method also gives only a rough idea of stable region especially for low modulation frequency  $\omega_v$  but generally overestimates the stability region for high frequency region.

## 5 CONCLUSION

We have transformed the synchrotron equation of motion in the QI regime into a universal Weierstrass equation, where the solution is expressed in Jacobian elliptic function. The phase space coordinates are expanded in action-angle variables. The strength function vanishes at the center of bucket and at the separatrix. Higher harmonic parametric resonances become more important near the separatrix. The effective damping coefficient  $A$  for the QI Hamiltonian is proportional to  $|\eta_0|^{-1/2}$ . And the effective modulation amplitude  $B$  is proportional to  $|\eta_1|/|\eta_0|^{3/2}$  (it is particularly enhanced). For rf phase modulation, the Melnikov integral method is a measure of rough estimation of the transition to global chaos only for  $\omega_m \leq 2$ . The role of parametric resonances in transition to chaos was identified for rf phase modulation. For  $\omega_m \geq 2$ , the stability is mainly determined by the 1:1 parametric resonance. For  $\omega_m \leq 2$ , the 2:1 parametric resonance on top of the 1:1 resonance makes the SFP of the 1:1 resonance unstable and bifurcate (Mathieu instability). A sequence of period-two bifurcation enroute to global chaos is a characteristic for  $\omega_m \leq 2$ . The effects of rf voltage modulation of QI dynamical system turns out to be insensitive.

## 6 REFERENCES

- [1] C. Pelligrini and D. Robin, Nucl. Inst. Methods, A **301**, 27 (1991).
- [2] D. Robin, E. Forest, C. Pelligrini, A. Amiry Phys. Rev. E **48**, 2149 (1993); H. Bruck *et al.*, IEEE Trans. on Nucl. Science NS**20**, 822 (1973).
- [3] L. Liu *et al.*, Nucl. Inst. and Methods **A329**, 9 (1993).
- [4] H. Hama, S. Takano and B. Isoyama, Nucl Inst. and Methods **A329**, 29 (1993). S. Takano, H. Hama and G. Isoyama, Japan J. of Appl. Phys. **32**, 1285 (1993).
- [5] A. Nadji *et al.*, Proceedings of the 4th European particle accelerator conference, p. 128 (1994).
- [6] D. Robin, H. Hama, and A. Nadji, Lawrence Berkeley Tech-note LBL-37758 (1995).
- [7] D. Robin *et al.*, SLAC-PUB-95-7015 (1995).
- [8] A. Riabko *et al*, Phys. Rev. E **54**, 815 (1996).
- [9] D. Jeon *et al*, Phys. Rev. E **54**, 4192 (1996).
- [10] M. Bai *et al*, Phys. Rev. E **55**, 3493 (1997).